International Journal of Heat and Mass Transfer 52 (2009) 1–8

Contents lists available at ScienceDirect

International Journal of Heat and Mass Transfer

journal homepage: www.elsevier.com/locate/ijhmt

Conjugate heat transfer in an enclosure under the condition of internal mass transfer and in the presence of the local heat source

G.V. Kuznetsov, M.A. Sheremet *

Thermal Power Engineering Faculty, Tomsk Polytechnic University, 30, Lenin Avenue, 634050 Tomsk, Russia
Faculty of Mechanics and Mathematics, Tomsk State University, 36, Lenin Avenue, 634050 Tomsk, Russia

ARTICLE INFO

Available online 25 August 2008

Keywords:
Conjugate heat transfer
Natural convection
Unsteady flow
Enclosures
Numerical simulation

ABSTRACT

Conjugate convective–conductive heat transfer in a rectangular enclosure under the condition of mass transfer within cavity with local heat and contaminant sources is numerically investigated. Mathematical model, describing a two-dimensional and laminar natural convection in a cavity with heat-conducting walls, is formulated in terms of the dimensionless stream function, vorticity, temperature and solute concentration. The main attention is paid to the effects of Grashof number (*Gr*), Buoyancy ratio (*Br*) and transient factor on flow modes, heat and mass transfer.

1. Introduction

Natural convection as one of heat and mass transport processes, has vital importance in many phenomena observed both in an environment [1], and in a man-made ecosystem [1–6]. The engineering applications including designing of the microelectronic equipment [7,8], creation of the optimal modes of passive ventilation [9,10] are just some examples of these phenomena.

The investigation of conjugate heat transfer of natural convection and conduction in enclosures is the most specific and detached class of problems [11,12]. There are few papers concerning the given subjects. This fact is explained by the laborious mathematical simulation. One can not but agree with wide engineering applications of conjugate heat transfer problems such as heat transfer in building elements [13] and solar collectors, cooling of the electronic equipment due to free convection, etc. The recent researches in the given area are mostly devoted to the substantiation of the importance of the conjugate heat transfer analysis both in two-dimensional [12,14–17], and in three-dimensional [7,18] problems. Some papers consider configurations containing either uniformly distributed heat source [12], or the local heat-generating conducting body [18]. A constant temperature or a constant heat flux are set on external borders of the decision area. In practice Newton's conditions taking into account convective–radiative heat exchange with an environment are the most adequate conditions on external borders during the analysis of the technical equipment.

A combined influence of an environment, local heat source and solid phase elements with final heat conduction coefficient was analysed in [19,20]. The typical distributions of the hydrodynamic and thermal characteristics proving conjugate problem and essential interference of both natural convection in an enclosure and conduction in solid phase elements have been received. The present work is a logical continuation of the above investigations [19,20], but taking into account convective mass transfer.

The objective of this work is the mathematical simulation of conjugate convective–conductive heat transfer in an enclosure due to the local heat and contaminant sources and convective–radiative heat exchange with an environment.

2. Analysis

The physical model of transient conjugate heat and mass transfer and the coordinate system under consideration are schematically shown in Fig. 1.

The system considered in this paper consists of rectangles with different sizes. A heat source, located in the bottom of the decision region, is characterized by a constant temperature during the whole process. A contaminant source with constant concentration is disposed in the right part of the heat source surface. The length of the contaminant source is denoted $l \neq 0$, but the thickness of that is assumed to be a negligible quantity. Horizontal walls ($y = 0$, $y = L_y$) and a vertical wall ($x = L_x$) of the final thickness, forming the gas cavity, are assumed adiabatic from outside. Convective–radiative heat exchange with an environment is modeled on the outer boundary $x = 0$.

* Corresponding author. Tel.: +7 3822 412 462; fax: +7 3822 529 740.
E-mail address: Michael-sher@yandex.ru (M.A. Sheremet).

0017-9310/$ - see front matter © 2008 Elsevier Ltd. All rights reserved.
doi:10.1016/j.ijheatmasstransfer.2008.06.034

Nomenclature

a thermal diffusivity
$A = \frac{-\left(\frac{D\cdot\Delta C}{\rho\cdot L\cdot\sqrt{g\beta\Delta TL}}\right)}{1-\left(\frac{\xi_{cs}\cdot\Delta C+C_0}{\rho}\right)}$ the dimensionless group describing interprocess convection communications caused by the concentration gradient and by the diffusion transfer
$Bi = \alpha L/\lambda$ Biot number
$Br = (\beta_C\Delta C)/(\beta\Delta T)$ buoyancy ratio
C_0 initial solute concentration
C_{cs} solute concentration on contaminant source
D solutal diffusivity
$Fo = at_0/L^2$ Fourier number
g_x acceleration of gravity (horizontal projection)
g_y acceleration of gravity (vertical projection)
$Gr = g_y\beta\Delta TL^3/\nu^2$ Grashof number
L length of the gas cavity
L_x length of the enclosure
L_y height of the enclosure
$m_{cs} = C_{cs}/\rho$ mass concentration
$N = \varepsilon\sigma L(\Delta T)^3/\lambda$ Stark number
$Pr = \nu/a$ Prandtl number
$Sc = \nu/D$ Schmidt number
t time
t_0 time scale
T_0 initial temperature
T_e environmental temperature
T_{hs} temperature on heat source
u velocity in the horizontal direction
U dimensionless velocity in the horizontal direction
v velocity in the vertical direction
$v_{\bar{y}}$ the normal velocity component at the contaminant source ($y = \bar{y}$)
V dimensionless velocity in the vertical direction
V_0 velocity scale
x horizontal Cartesian coordinate
X dimensionless horizontal Cartesian coordinate
y vertical Cartesian coordinate
Y dimensionless vertical Cartesian coordinate

Greek symbols
α heat transfer factor
β coefficient of volumetric thermal expansion
β_C coefficient of volumetric solutal expansion
$\Delta = \frac{\partial^2}{\partial X^2} + \frac{\partial^2}{\partial Y^2}$ Laplacian
ΔC concentration difference
ΔT temperature difference
ε specific emissivity factor
Θ dimensionless temperature
λ thermal conductivity
$\lambda_{ij} = \lambda_i/\lambda_j$ thermal conductivity ratio
ν kinematic viscosity
ξ dimensionless concentration
ρ density
σ Stephen–Boltzman constant
τ dimensionless time
ψ stream function
ψ_0 stream function scale
Ψ dimensionless stream function
ω vorticity
ω_0 vorticity scale
Ω dimensionless vorticity

Subscripts
i number of the decision region element (Fig. 1)
cs contaminant source
hs heat source
e environment

It is assumed in the analysis that the thermophysical properties of the solid phase elements and of the gas are independent of temperature, and the flow is laminar. The fluid is Newtonian, incompressible, and the Boussinesq approximation is valid. The fluid motion and heat transfer in the cavity are supposed to be two-dimensional. Radiation heat exchange between the walls is neglected in comparison with convection. The fluid is presumed to be radiatively non-participating. Viscous heat dissipation in the fluid is assumed to be negligible in comparison with conduction and convection. Soret and Dufour thermodynamical effects are neglected.

The heat and mass transfer process in considered area (Fig. 1) is described by transient two-dimensional equations under Boussinesq approach into the cavity [11], by the non-stationary equation of mass diffusion on the basis of Fick's law [21] and by the non-stationary two-dimensional equation of heat conductivity for the solid phase elements [22] with nonlinear boundary conditions.

The mathematical model was formulated in terms of the dimensionless variables such as stream function, vorticity, temperature and solute concentration.

The length of the cavity along x axis was chosen as a scale distance. For reduction to dimensionless form of the system of the equations the following correlations were used:

$$X = x/L,\quad Y = y/L,\quad \tau = t/t_0,\quad U = u/V_0,\quad V = v/V_0,\quad \Theta = (T - T_0)/\Delta T,$$
$$\xi = (C - C_0)/\Delta C,\quad \Psi = \psi/\psi_0,\quad \Omega = \omega/\omega_0,$$

where $V_0 = \sqrt{g_y\beta\Delta TL}$, $\Delta T = T_{hs} - T_0$, $\Delta C = C_{cs} - C_0$, $\psi_0 = V_0L$, $\omega_0 = V_0/L$.

The governing equations of convective heat and mass transfer in dimensionless form become:

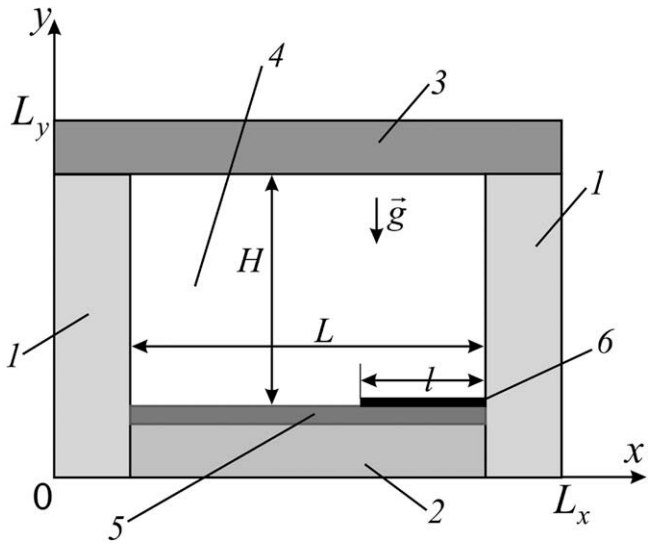

Fig. 1. A scheme of the system: *1*, *2*, *3* – solid phase elements; *4* – fluid; *5* – heat source; *6* – pollutant source.

- in the cavity (*4* in Fig. 1)

$$\frac{\partial \Omega}{\partial \tau}+\frac{\partial \Psi}{\partial Y}\frac{\partial \Omega}{\partial X}-\frac{\partial \Psi}{\partial X}\frac{\partial \Omega}{\partial Y}=\frac{1}{\sqrt{Gr}}\left(\frac{\partial^2 \Omega}{\partial X^2}+\frac{\partial^2 \Omega}{\partial Y^2}\right)+\left(\frac{\partial \Theta}{\partial X}+Br\frac{\partial \xi}{\partial X}\right), \quad (1)$$

$$\Delta \Psi=-\Omega, \quad (2)$$

$$\frac{\partial \Theta}{\partial \tau}+\frac{\partial \Psi}{\partial Y}\frac{\partial \Theta}{\partial X}-\frac{\partial \Psi}{\partial X}\frac{\partial \Theta}{\partial Y}=\frac{1}{\sqrt{Gr}\cdot Pr}\left(\frac{\partial^2 \Theta}{\partial X^2}+\frac{\partial^2 \Theta}{\partial Y^2}\right), \quad (3)$$

$$\frac{\partial \xi}{\partial \tau}+\frac{\partial \Psi}{\partial Y}\frac{\partial \xi}{\partial X}-\frac{\partial \Psi}{\partial X}\frac{\partial \xi}{\partial Y}=\frac{1}{\sqrt{Gr}\cdot Sc}\left(\frac{\partial^2 \xi}{\partial X^2}+\frac{\partial^2 \xi}{\partial Y^2}\right), \quad (4)$$

- for the solid phase elements

$$\frac{1}{Fo_i}\frac{\partial \Theta_i}{\partial \tau}=\Delta \Theta_i, \quad i=\overline{1,3}. \quad (5)$$

Initial and boundary conditions for the formulated problem (1)–(5) look like:

Initial conditions:

$\Psi(X,Y,0)=0$, $\Omega(X,Y,0)=0$,

$\Theta(X,Y,0)=0$, $\xi(X,Y,0)=0$ with the exception of heat and contaminant sources, on which during the whole process $\Theta=\xi=1$, respectively.

Boundary conditions:

- at $X=0$ the conditions considering heat exchange with an environment due to convection and radiation are realized

$$\frac{\partial \Theta_i(X,Y,\tau)}{\partial X}=Bi_i\cdot\Theta_i(X,Y,\tau)+Bi_i\cdot\frac{T_0-T_e}{T_{hs}-T_0}+Q_i,$$

$$\text{under } Q_i=N_i\cdot\left[\left(\Theta_i(X,Y,\tau)+\frac{T_0}{T_{hs}-T_0}\right)^4-\left(\frac{T_e}{T_{hs}-T_0}\right)^4\right];$$

  where $i=1, 3$ according to Fig. 1;
- adiabatic conditions are set on other external borders

$$\frac{\partial \Theta_i(X,Y,\tau)}{\partial X^k}=0, \qquad \text{where } X^1\equiv X, \quad X^2\equiv Y; \quad i=\overline{1,3};$$

- at all parts of the decision region where there is an interface of materials with various thermophysical characteristics, conditions of 4th sort were accomplished

$$\Theta_i=\Theta_j, \quad \frac{\partial \Theta_i}{\partial X^k}=\lambda_{j,i}\frac{\partial \Theta_j}{\partial X^k}, \qquad i,j=\overline{1,4}, \quad i\neq j, k=1,2;$$

- at internal solid–fluid interface parallel to an axis 0*X*:

$$\Psi=\frac{\partial \Psi}{\partial Y}=\frac{\partial \xi}{\partial Y}=0, \quad \Theta_3=\Theta_4, \quad \frac{\partial \Theta_3}{\partial Y}=\lambda_{4,3}\frac{\partial \Theta_4}{\partial Y};$$

- at internal solid–fluid interface parallel to an axis 0*Y*:

$$\Psi=\frac{\partial \Psi}{\partial X}=\frac{\partial \xi}{\partial X}=0, \quad \Theta_1=\Theta_4, \quad \frac{\partial \Theta_1}{\partial X}=\lambda_{4,1}\frac{\partial \Theta_4}{\partial X}.$$

As is known [23], due to the local contaminant source the normal velocity component at the contaminant source is distinct from zero and it is calculated by the formula:

$$v_{\bar{y}}=\frac{-\left(\frac{D}{\rho}\right)\left(\frac{\partial C_{cs}}{\partial y}\right)_{y=\bar{y}}}{1-m_{cs,\bar{y}}}=\frac{-\left(\frac{D}{\rho}\right)\left(\frac{\partial C_{cs}}{\partial y}\right)_{y=\bar{y}}}{1-\left(\frac{C_{cs}}{\rho}\right)_{y=\bar{y}}}. \quad (6)$$

The formula (6) in dimensionless form becomes: $V_{Y=0.2}=A\cdot\left(\frac{\partial \xi}{\partial Y}\right)_{Y=0.2}$.

Therefore, boundary condition at the contaminant source ($Y=0.2$, $0.93\leqslant X\leqslant 1.215$):

$$\xi=\Theta=1, \quad \frac{\partial \Psi}{\partial Y}=0, \quad \Psi(X)=-A\cdot\int_{0.93}^{X}\frac{\partial \xi}{\partial Y}\,dX.$$

The problem (1)–(5) with the corresponding boundary and initial conditions has been solved by the finite difference method [24,25].

The solution method has been tested on several model problems such as natural convection of air in a square cavity and conjugate natural convection in a square enclosure. The comparison of the results with those of other authors [26,27] has shown that the method used leads to rather good coordination.

3. Results and discussion

Numerical simulation of the boundary problem (1)–(5) with corresponding initial and boundary conditions are realized with following values of geometrical ratios: $L_x/L=1.43$, $L_y/L=1.0$, $H/L=0.65$, $l/L=0.3$. Dimensionless groups are $Gr=10^5$–10^7, $Pr=Sc=0.702$, $Br=1{,}6$, describing typical modes of natural convective heat and mass transfer. The thermophysical properties of solid phase elements (*1–3* in Fig. 1) are identical: $Bi_1=Bi_3=88.7$, $N_1=N_3=0.0018$. Fourier numbers of solid phase elements are equal: $Fo_1=Fo_2=Fo_3=1.4\times10^{-7}$. Dimensionless defining temperatures and concentration accepted following values: $\Theta_e=-1$, $\Theta_{hs}=\xi_{cs}=1$, $\Theta_0=\xi_0=0$. The main attention was paid to the effects of the strength of heat source (*Gr*), the strength of contaminant source (*Br*) and transient factor on distributions of the basic characteristics of the investigated process.

3.1. Effect of Grashof number

To consider only the effect of *Gr* on the conjugate natural convection the other parameters are kept fixed at $Br=1$, $\tau=2\times10^4$. Fig. 2 shows streamlines, a vorticity field, a temperature field and a concentration field. Arrows on streamlines indicate a direction of the fluid motion.

Two convective cells are formed in the cavity in convective heat and mass transfer mode, corresponding to $Gr=10^5$ (Fig. 2a). The main eddy represents the motion of the gas mass counter-clockwise. One occupies a greater area in comparison with the small circulating flow located directly in a zone above the contaminant source. The presented orientation of gas flow characterizes asymmetric property of the investigated process well enough. The latter is associated with nonlinear influence of an environment on the decision region that is reflected in the distribution of isotherms. The propulsion of the reduced temperature wave from $X=0$ is noticed in the left solid phase element. The latter leads to the appearance of the descending cold gas flow. The formation of ascending gas streams above the contaminant source is explained by the presence of essential temperature and concentration gradients which are components of buoyancy force. The interaction of gas convective flows and solid phase elements can be characterized by the vorticity field. The vorticity defined as $\Omega=curl_z\vec{V}$, describes the distribution of agitations from solid phase elements which form the certain velocity boundary layer at walls surface. In the center of the gas cavity the uniform vorticity core, describing circulating gas flow, is formed. Under the conditions of natural convection the velocity boundary layer is inseparably connected with a thermal boundary layer. It should be noted, that the thickness of the thermal boundary layer coincides with the thickness of the velocity boundary layer in case of free convection [28]. But by consideration of combined heat and mass transfer the latter statement can be broken in connection with flow generated not only by the temperature gradient, but also by the concentration gradient.

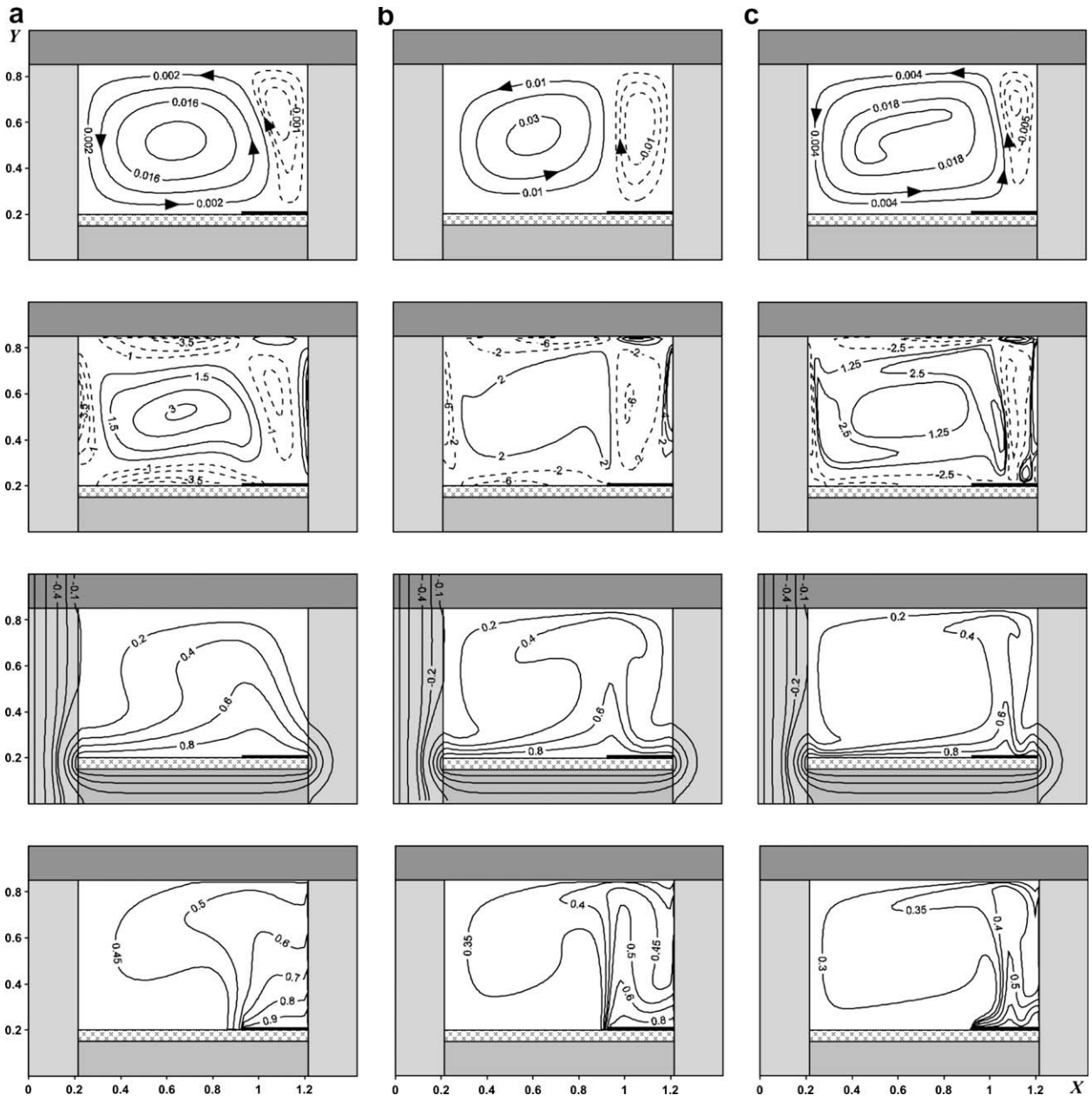

Fig. 2. Typical stream lines Ψ, vorticity field Ω, temperature field Θ and concentration field ξ at $Br = 1$, $\tau = 2 \times 10^4$: (a) $Gr = 10^5$, (b) $Gr = 10^6$, (c) $Gr = 10^7$.

The distribution of isotherms in the gas cavity occurs non-uniformly, with the thermal "plume" displaced into a zone of the contaminant source. The configuration of isotherms implicitly reflects the presence of convective cells in the gas cavity. A break of the isotherm, corresponding to dimensionless temperature equals to 0.2, characterizes the presence of the descending cold flow at the left solid phase element.

The interface of low and high temperature waves in the left wall leads to the break of isotherms and to the non-uniform formation of the thermal field. At the same time the concentration field in the gas cavity is induced by the concentration gradient, leading to the appearance of the diffusion "plume" above the contaminant source. The latter leads to the concentration dispersion along the surface of the right solid phase element with the subsequent break in the direction of the main circulating flow.

The increase in Grashof number to $Gr = 10^6$ (Fig. 2b) leads to the modification of analyzed variables fields. Increase in Gr in the gas cavity is reflected in the growth of the circulating flow speed. The main convective cell diminishes in sizes. It is possible to explain by the formed thermal "plume" above the left border of the contaminant source. At the same time a width of the thermal "plume" (a distance between the isotherm branches corresponding to dimensionless temperature 0.4) is great, that leads to the increase in eddy scales, located at the right solid phase element. The modification of the vorticity field is connected with the increase in magnitude of the vorticity and with some distortion of the central core. Thus it is possible to evolve the region of ascending warm streams in the temperature field as an original convective column. The increase in the role of volumetric forces leads to intensive warming-up of the gas cavity (the isotherm corresponding to dimensionless temperature 0.2 occurs in a greater area in comparison with mode at $Gr = 10^5$). The curvatures of the mentioned isotherm in the zone of the left and right walls characterize the presence of the descending gas streams of the lowered

temperature that is proved by the distribution of stream lines. Also it is necessary to note the "extrusion" of the isotherm, corresponding to dimensionless temperature −0.1, from the gas cavity onto the wall border in comparison with Fig. 2a. The concentration field is being essential by changed. As in the case of the distribution of isotherms, the formation of more precise diffusion "plume" takes place here.

At $Gr = 10^7$ an interesting flow situation is observed. There is again an increase in scales of the main convective cell which undergoes serious structural changes. At the same time the velocity in the center of this cell decreases in comparison with natural convection at $Gr = 10^6$. It is explained by the fact that the increased role of mass forces influences on the flow structure. The vorticity field evidently confirms the thesis formulated above. Analyzing the distribution of isotherms, it is possible to emphasize displacement and reduction of the thermal "plume" width that has led to narrowing of the right convective cell region. The diffusion "plume" is also displaced to the center of the contaminant source. Coordinate maxima of constant concentration lines decrease to bottom of the gas cavity.

The given analysis can integrally be presented in the form of dependences on Grashof number of average Nusselt number and Sherwood number at characteristic solid–fluid interface: $Nu_{avg} = \int_{0.215}^{1.215} \left|\frac{\partial\Theta}{\partial Y}\right|_{Y=0.85} dX$, $Sh_{avg} = \frac{1}{0.285}\int_{0.93}^{1.215} \left|\frac{\partial\xi}{\partial Y}\right|_{Y=0.2} dX$.

The presented graphic dependences of average Nusselt number describe the integrated heat transfer factor at $Y = 0.85$ with Grashof number. Fig. 3 evidently shows the characteristic growth of the heat transfer intensity in a range of change of the defining parameter $10^5 \leqslant Gr \leqslant 10^7$. The use of correlation is very convenient in carrying out applied calculations. It is possible to interpret graphic dependence (Fig. 3a) mathematically as follows:

$$Nu_{avg} = 0.18 \cdot Gr^{0.18} \quad \text{at } Br = 1, 6.$$

A similar growth of the mass transfer intensity is reflected by dependences on Fig. 3b. At the same time average Sherwood number (or average diffusion Nusselt number) defines the integrated mass transfer factor. The corresponding correlation will become:

$$Sh_{avg} = 0.18 \cdot Gr^{0.28} \quad \text{at } Br = 1;$$
$$Sh_{avg} = 0.14 \cdot Gr^{0.31} \quad \text{at } Br = 6.$$

3.2. Effect of buoyancy ratio

Buoyancy ratio reflects the relative strength of the contaminant source compared to the heat source. When the heat source described by Gr is kept fixed, the change of the contaminant source is represented by the parameter Br. Thus it is necessary to note, that the growth of buoyancy ratio corresponds to the increase in the role of the diffusion gradient in formation of flow modes. The distributions of streamlines, vorticity field, temperature field and concentration field at various Grashof numbers $10^5 \leqslant Gr \leqslant 10^7$ and $Br = 6$ are presented in Fig. 4.

The comparison of Fig. 2 with Fig. 4 allows to distinguish the principal characteristics and features of the investigated process at the change of buoyancy ratio.

The increase in buoyancy ratio up to $Br = 6$ in the convective heat and mass transfer mode, corresponding to $Gr = 10^5$, leads to the growth of the sizes and velocities of the main convective cell. The eddy, located at the right solid phase element (at $Br = 1$), dissipates. The vorticity field also changes. There is a lengthening of the central core along an axis $0X$, that leads to the disappearance of the vortex structures at the right solid phase element. The temperature field can be added to the presented hydrodynamical picture. The comparison of Fig. 2a with Fig. 4a shows displacement of the thermal "plume" (at $Br = 6$) in the zone of the right wall. Also there is a decrease in the coordinate maxima corresponding to isotherms, located above the contaminant source.

The presented changes are connected with the increase in a part of the buoyancy force caused by the diffusion gradient. The increase in buoyancy ratio leads to the intensification of the mass transfer process (Fig. 3).

In the mode corresponding to $Gr = 10^6$ (Fig. 4b) the aggregation of the convective cells and essential modification of both the vorticity field and the temperature field take place. The thermal "plume" is displaced to the right wall. The mean temperature in the gas cavity goes down. The diffusion "plume" also approaches to the right solid phase element. The reason is the absence of the circulating flow in the right part of the gas cavity. The latter leads to the obvious contaminant transport along all cavity.

The comparison of Fig. 4c with Fig. 2c allows to distinguish the main zones and scales of the buoyancy ratio influence.

3.3. Effect of transient factor

The dependence of the sought quantities on time essentially amends the formation of the hydrodynamical, thermal and diffusion flow modes. The transient factor is determined not only by dynamics of the sought quantities in the gas cavity connected with flow origin (from a quiescent state during the initial moment of time), but by the formation of the main vortex structures and transition to the some quasistationary mode. But also this factor is defined by the thermal sluggishness of the solid phase elements,

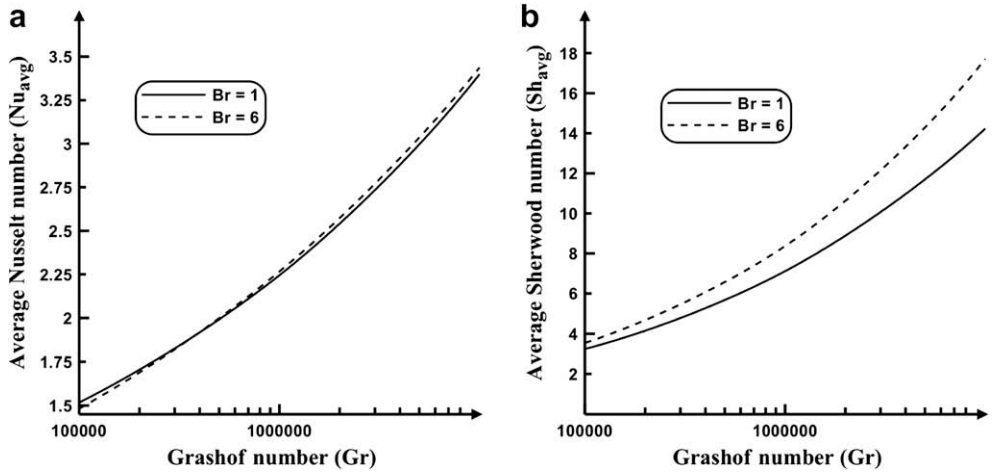

Fig. 3. (a) Variations of average Nusselt number and (b) average Sherwood number with Grashof number for $\tau = 5 \times 10^4$.

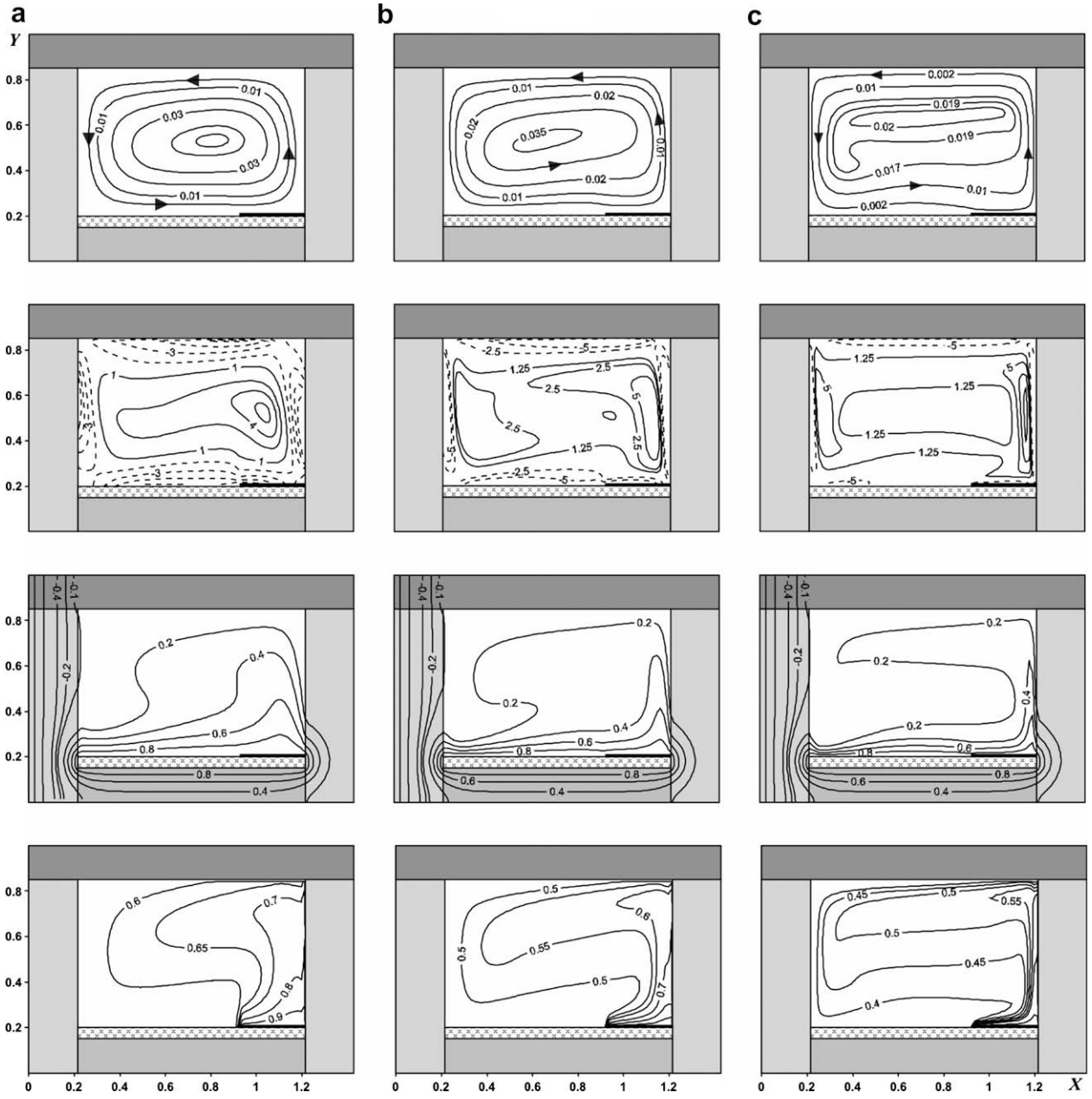

Fig. 4. Typical stream lines Ψ, vorticity field Ω, temperature field Θ and concentration field ξ at $Br = 6$, $\tau = 2 \times 10^4$: (a) $Gr = 10^5$, (b) $Gr = 10^6$, (c) $Gr = 10^7$.

owing to conductive heat transfer. The thesis formulated above selects a class of the conjugate problems in the specific structure. The conjugate statement allows to consider not only the temperature change at heat flux at the solid walls, having final thickness. But also the conjugate statement allows to consider the transient factor which influences on the distribution of both local, and integrated characteristics.

Fig. 5 shows the dynamics of hydrothermodiffusion fields formation at $Gr = 10^7$, $Br = 1$.

At $\tau = 10^4$ (Fig. 5a) two convective cells and two recirculation flows caused both by geometry of the decision region and by the time period corresponding to a stage of vortex structures origin are formed in the gas cavity. The formed vorticity core in the center of the gas cavity corresponds to the considered initial stage. Appearing hydrodynamical structures interact with the temperature and concentration fields. The thermal "plume" is formed on the left boundary of the contaminant source. The propulsion rate of the lowered temperature wave in the left solid phase element from the boundary $X = 0$ is less than the convective heat transfer rate in the gas cavity. Therefore, the isotherm corresponding to dimensionless temperature 0.2 covers all gas cavity. Similarly there is a formation of the diffusion "plume".

The increase in a time interval ($\tau = 3 \times 10^4$) leads to modification of both the flow structures and the temperature and diffusion fields. In the gas cavity there is a confinement of the vortex flow located on the right solid phase element. It leads to the local symmetry of the central vorticity field ($\Omega > 1.25$). The thermal "plume" is displaced to the right wall. The lowered temperature wave achieves the gas cavity (the isotherm corresponding to dimensionless temperature -0.1 is on the boundary $X = 0.215$). Also the most intensive descending cold streams on this boundary are observed. This is proved by the distortion of the isotherm corresponding to

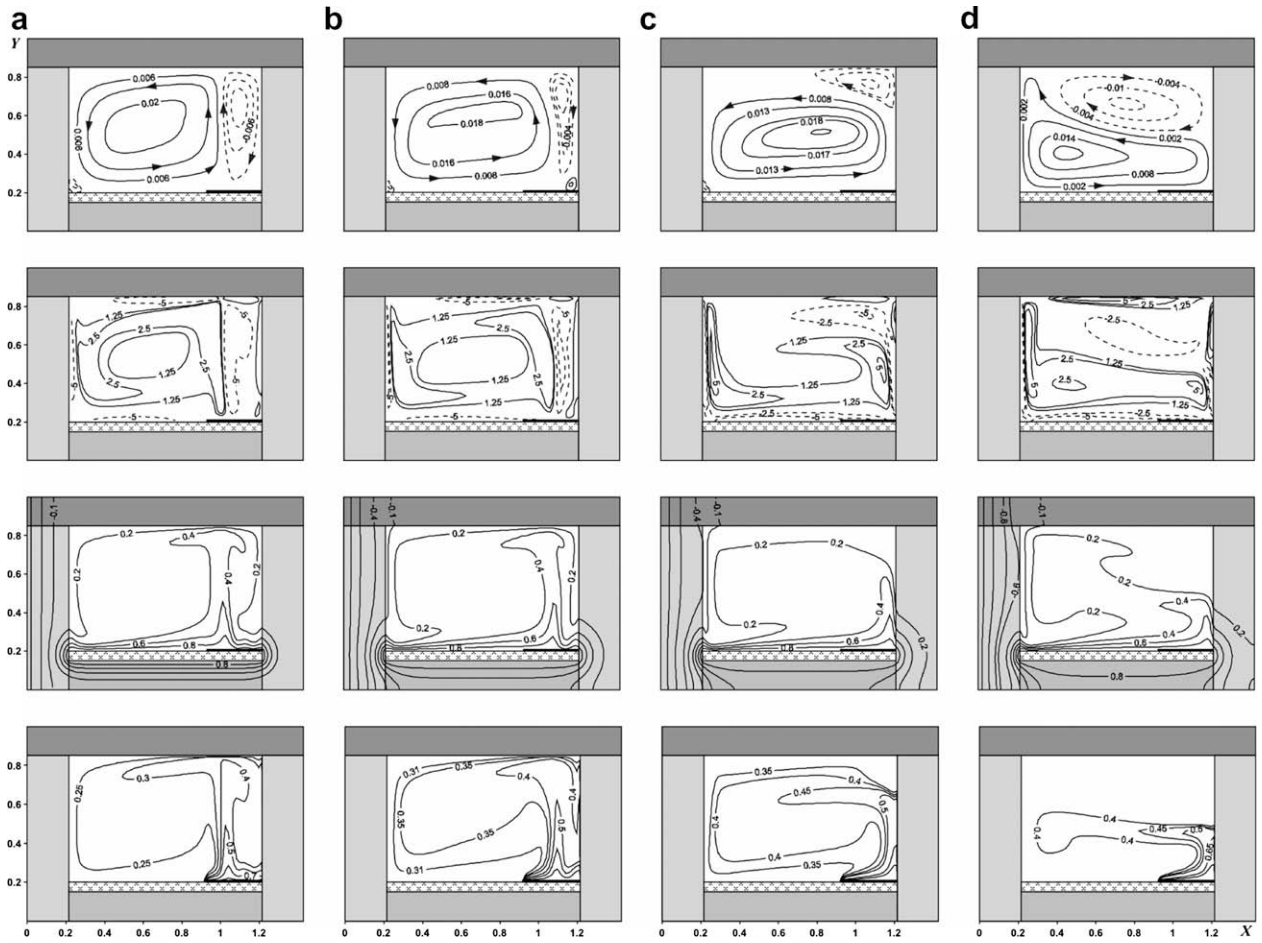

Fig. 5. Effect of transient factor on the stream lines Ψ, the vorticity field Ω, the temperature field Θ and the concentration field ξ at $Gr = 10^7$, $Br = 1$: (a) $\tau = 10^4$, (b) $\tau = 3 \times 10^4$, (c) $\tau = 4 \times 10^4$, (d) $\tau = 5 \times 10^4$.

dimensionless temperature 0.2 in zone of the left bottom corner of the gas cavity. The concentration field changes, namely, the diffusion "plume" also is displaced to the right wall.

At $\tau = 4 \times 10^4$ (Fig. 5c) an essential modification of the right convective cell occurs, namely, it degenerates into the circulating flow occupying the right top corner. Such behavior of the convective cell leads to essential reconfiguration of the vorticity field, namely, the central core dissipates. The thermal "plume" is interfaces to a surface of the right wall that leads to the decrease in a coordinate maximum of the isotherm corresponding to dimensionless temperature 0.4. The lowered temperature wave continues to advance into the gas cavity, that most precisely is represented in the zone of the bottom left corner. The diffusion "plume" also attaches to the right wall and somehow is deformed by the circulating flow located in the top right corner.

At $\tau = 5 \times 10^4$ (Fig. 5d) the increase in the sizes and the intensity of the vortex flow located in the top right corner occurs. The flow formed thus leads to the essential modification of the vorticity field as well as the temperature and the concentration fields.

Fig. 6 shows the dependences of the integrated parameters describing heat and mass transfer processes on dimensionless time for various values of Grashof number and buoyancy ratio.

The dependences (Fig. 6) describe the essential features and the most specific aspects of each of analyzed flow and heat/mass transfer modes.

The Boussinesq approximation for heat transfer and analogy between heat and mass transfer processes were used for the description of conjugate heat and mass transfer in the considered analysis. The density was assumed to be linearly dependent on concentration and temperature at definition of the buoyancy force in the motion equation. This approximation is exact enough [23] for both dropping liquid and gases at small values of temperature and diffusion differences. The Boussinesq approximation $\Delta\rho = \rho\beta(T - T_0)$ is known to be a good estimation of density dependence on temperature under condition of $\beta(T - T_0) \ll 1$. The approach $\Delta\rho = \rho\beta_C(C - C_0)$ is obtained from similar considerations to be a precisely enough idea of the density dependence on concentration under condition of $\beta(C - C_0) \ll 1$.

The normal velocity component on the mass source is known to be differing from zero in the presence of intensive mass transfer. This condition has been realized in the present research. But at the Boussinesq approximation this condition slightly changes physical problem definition. Therefore, at the analysis of possible critical operating modes of the investigated object at greater temperature and concentration differences the Boussinesq approximation is insufficiently proved.

The temperature and concentration differences were small enough in the analyzed heat and mass transfer process, that first of all in practice relates, for example, to typical operating modes of units and blocks of the radio-electronic equipment. Therefore, use of the Boussinesq approximation and analogy between heat and mass transfer processes here is pertinent. One of the proofs of the latter is that the presence of non-zero normal velocity component on the mass source leads to insignificant changing both local (velocity, temperature and concentration fields) and integral (average Nusselt number and Sherwood number) characteristics

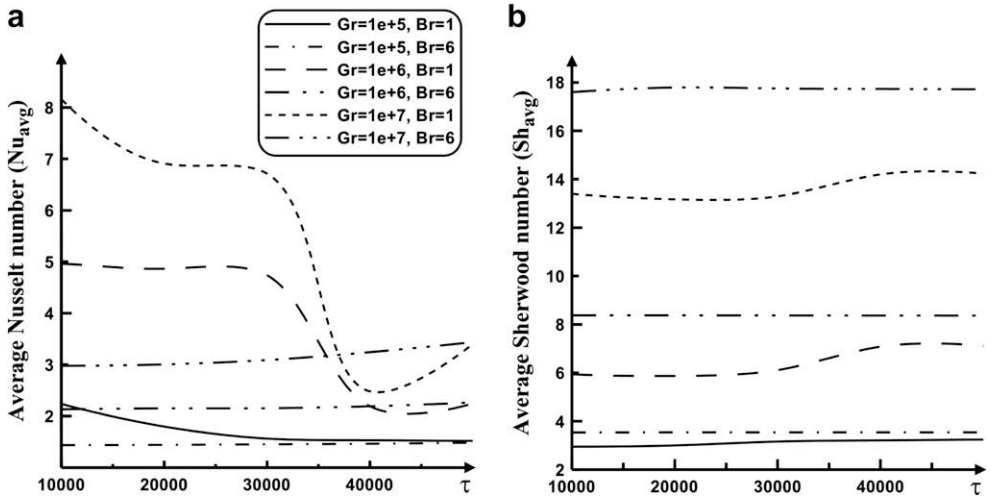

Fig. 6. (a) Variations of average Nusselt number and (b) average Sherwood number with dimensionless time at $Gr = 10^5$–10^7, $Br = 1, 6$.

of the investigated process in comparison with the zero normal velocity component.

4. Conclusions

Conjugate heat transfer in a rectangular enclosure on the assumption of internal mass transfer and in the presence of local heat and contaminant sources is numerically investigated in the present work. The influence of an environment was taken into account in conditions of the convective-radiation heat exchange on one of external boundaries of the decision region. Typical distributions of the stream lines, the vorticity field, the temperature field and the concentration field in a wide range of the defining parameters $10^5 \leqslant Gr \leqslant 10^7$; $Br = 1, 6$; $Pr = Sc = 0.702$ have been received. Efforts have been made to consider how the main factors (Grashof number, buoyancy ratio and transient factor) influence on the formation of the hydrothermodiffusion fields. It has been determined, that the increase in a diffusion processes role (Br) does not lead to an intensification of heat transfer (Fig. 3a). Nonlinear influence scales of an environment, owing to conduction in the solid walls limiting the gas cavity have been determined. The correlations describing the dependence of average Nusselt numbers and average Sherwood numbers on Grashof number have been received. The obtained correlations allow to carry out the computations of the integral heat/mass transfer factors at heat-conducting walls of final thickness and with the transient factor.

Acknowledgements

This work was supported by the Russian Foundation for Basic Research and Administration of Tomsk region (No. 05-02-98006, competition r_ob_a).

References

[1] A. Bejan, Convection Heat Transfer, Wiley, New York, 1982.
[2] P.H. Oosthuizen, J.T. Paul, Natural convection in a rectangular enclosure with two heated sections on the lower surface, Int. J. Heat Fluid Flow 26 (2005) 587–596.
[3] L. Adjlout, O. Imine, A. Azzi, M. Belkadi, Laminar natural convection in an inclined cavity with a wavy wall, Int. J. Heat Mass Transfer 45 (2002) 2141–2152.
[4] A.A. Mohamad, J. Sicard, R. Bennacer, Natural convection in enclosures with floor cooling subjected to a heated vertical wall, Int. J. Heat Mass Transfer 49 (2006) 108–121.
[5] E. Bilgen, Natural convection in cavities with a thin fin on the hot wall, Int. J. Heat Mass Transfer 48 (2005) 3493–3505.
[6] T.S. Chang, Y.L. Tsay, Natural convection heat transfer in an enclosure with a heated backward step, Int. J. Heat Mass Transfer 44 (2001) 3963–3971.
[7] A.G. Fedorov, R. Viskanta, Three-dimensional conjugate heat transfer in the microchannel heat sink for electronic packaging, Int. J. Heat Mass Transfer 43 (2000) 399–415.
[8] M. Alami, M. Najam, E. Semma, A. Oubarra, F. Penot, Electronic components cooling by natural convection in horizontal channel with slots, Energy Convers. Manage. 46 (2005) 2762–2772.
[9] G. Ziskind, V. Dubovsky, R. Letan, Ventilation by natural convection of a one-storey building, Energy Build. 34 (2002) 91–102.
[10] R. Letan, V. Dubovsky, G. Ziskind, Passive ventilation and heating by natural convection in a multi-storey building, Build. Environ. 38 (2003) 197–208.
[11] D.M. Kim, R. Viskanta, Study of the effects of wall conductance on natural convection in differently oriented square cavities, J. Fluid Mech. 144 (1984) 153–176.
[12] A. Liaqat, A.C. Baytas, Conjugate natural convection in a square enclosure containing volumetric sources, Int. J. Heat Mass Transfer 44 (2001) 3273–3280.
[13] O. Aydin, Conjugate heat transfer analysis of double pane windows, Build. Environ. 41 (2006) 109–116.
[14] A.A. Merrikh, J.L. Lage, Natural convection in an enclosure with disconnected and conducting solid blocks, Int. J. Heat Mass Transfer 48 (2005) 1361–1372.
[15] Q.-H. Deng, G.-F. Tang, Numerical visualization of mass and heat transport for conjugate natural convection/heat conduction by streamline and heatline, Int. J. Heat Mass Transfer 45 (2002) 2373–2385.
[16] J.R. Lee, M.Y. Ha, A numerical study of natural convection in a horizontal enclosure with a conducting body, Int. J. Heat Mass Transfer 48 (2005) 3308–3318.
[17] M.K. Das, K.S.K. Reddy, Conjugate natural convection heat transfer in an inclined square cavity containing a conducting block, Int. J. Heat Mass Transfer 49 (2006) 4987–5000.
[18] M.Y. Ha, M.J. Jung, A numerical study on three-dimensional conjugate heat transfer of natural convection and conduction in a differentially heated cubic enclosure with a heat-generating cubic conducting body, Int. J. Heat Mass Transfer 43 (2000) 4229–4248.
[19] G.V. Kuznetsov, M.A. Sheremet, Modelling of non-stationary heat transfer in closed area with a local heat source, Thermophys. Aeromech. 12 (2) (2005) 287–295.
[20] G.V. Kuznetsov, M.A. Sheremet, Conjugate heat transfer in a closed domain with a locally lumped heat-release source, J. Eng. Phys. Thermophys. 79 (1) (2006) 57–64.
[21] Q.-H. Deng, G. Zhang, Indoor air environment: more structures to see? Build. Environ. 39 (2004) 1417–1425.
[22] A.V. Lykov, Theory of Thermal Conductivity, Vysshaya shkola, Moscow, 1967.
[23] B. Gebhart, Y. Jaluria, R.L. Mahajan, B. Sammakia, Buoyancy-induced Flows and Transport, Hemisphere Publishing Corporation, 1988.
[24] P.J. Roache, Computational Fluid Dynamics, Hermosa Publishers, Albuquerque, 1976.
[25] C.A.J. Fletcher, Computational Techniques for Fluid Dynamics, vol. 2, Springer-Verlag, Berlin, Heidelberg, 1988.
[26] G. de Vahl Davis, Natural convection of air in a square cavity: a bench numerical solution, Int. J. Numer. Methods Fluids 3 (1983) 249–264.
[27] D.A. Kaminski, C. Prakash, Conjugate natural convection in a square enclosure effect of conduction on one of the vertical walls, Int. J. Heat Mass Transfer 29 (1986) 1979–1988.
[28] Yu.A. Sokovishin, O.G. Martynenko, Introduction in the Theory of Free Convective Heat Exchange, Leningrad State University, Leningrad, 1982.